Potential Challenges for the Restoration of Biscayne Bay (Florida, USA) in the Face of Climate Change Effects Revealed with Predictive Models

Vladimir J. Alarcon[1]
Anna C. Linhoss[2]
Christopher R. Kelble[3]
Paul F. Mickle[1]
Alexandra Fine[3, 4]
Enrique Montes[3, 4]

1. Northern Gulf Institute, MSU Science and Technology Center, 1021 Balch Blvd.
Stennis Space Center, MS 39529, USA

2. Department of Biosystems Engineering, Auburn University, 350 Mell St. Auburn, AL 36849, USA

3. Ocean Chemistry amd Ecosystems Division, NOAA Atlantic Oceanographic and Meteorological Laboratory, 4301 Rickenbacker Causeway, Miami, FL 33149, USA.

4. Cooperative Institute for Marine and Atmospheric Studies, University of Miami, USA.

for publication in

Ocean and Coastal Management

Abstract

Estuaries and coastal areas worldwide are rapidly changing, especially those adjacent to urban centers. Physical and ecological stresses are exacerbated by climate change (CC) and sea level rise (SLR). In this research, a salinity transport model for Biscayne Bay is presented. The model is used to estimate salinity under various scenarios of altered precipitation, increased salinity/temperature, and SLR. The simulated scenarios (based on prior studies and existing literature) assumed increases of 1.5°C in temperature, and 0.6 PSU in ocean salinity. Current precipitation was varied from -10% to +10%. SLR varied from +0.46 m to +2.18 m. The highest increase in bay salinity (worst-case scenario) occurred for 10% decrease in precipitation, and +2.18 m SLR. The lowest increase in salinity (mildest scenario) occurred for 10% increase in precipitation, and +0.46 m SLR. In the mildest scenario, a 50% increase in baseline freshwater inputs is needed to maintain currently observed Bay salinities. For the worst scenario, a 300% freshwater increase would be required. Current Everglades Restoration plans to restore the Bay salinity to "natural" conditions must consider the potential CC-induced effects simulated in this research. Present efforts may not be sufficient to even maintain current salinity conditions in Biscayne Bay. Increasing urban vegetation (urban greening), artificial groundwater recharge with treated wastewater, and decreasing water consumption, are proposed as management measures for reinforcing current and future restoration efforts.

Keywords: Salinity modeling, altered precipitation, increased temperature, sea level rise, EFDC

Highlights

- Future simulated scenarios predict that salinity will increase in Biscayne Bay.
- For the mildest scenario, 50% freshwater increase would maintain current salinities.
- For the worst scenario, 300% freshwater increase would maintain current salinities.
- SLR and CC impacts should be considered in coastal waters restoration efforts.

Software availability

- Name of software: EFDC+ Explorer Modeling System (EEMS)
- Developers: Original software (EFDC): John Hamrick (1988). DSI LLC (https://dsi.llc/eems) has upgraded the original software to EFDC+ Explorer Modeling System (EEMS) (1998 to current).
- Hardware required: PC, or computer cluster (MPI/OpenMP hybrid)
- Software required: Windows or Linux.
- Availability: Open source: https://github.com/dsi-llc/EFDCPlus. Commercial software: https://www.eemodelingsystem.com/ee-modeling-system/efdc-plus/overview
- Cost: Depends on type of license
- Program language: FORTRAN.
- First available: 1988.

1. Introduction

The combined effects of climate change (CC) and sea level rise (SLR) can have synergistic impacts on coastal communities and ecosystems (Basack et al., 2022; White and Kaplan, 2017). Over the last century, estuaries worldwide have seen unprecedented stress and changes in their physical and ecological dynamics, especially those adjacent to urbanized centers and ports (Pareja-Roman and Chant 2023). Changes in estuarine tidal amplitude have been ubiquitous, often in response to wetland reclamation, channel dredging, and other environmental changes (Talke et al., 2020). Global CC-induced shifts in watershed dynamics, river discharge, tides, sea level rise (SLR), increasing temperatures, and anthropogenic interventions have a significant impact on the coupled physical and ecological dynamics of estuarine systems (Pareja-Roman and Chant 2023). SLR threatens estuaries with a range of interconnected and cascading coastal hazards and risks, including enhanced coastal flooding as well as changes or losses of intertidal wetlands with adverse implications for biodiversity, ecosystem services and human livelihoods (Hinkel et al., 2023, Khojaste et al., 2021, Talke et al., 2020).

A multidecadal study on linear trends of global ocean salinity patterns (Durack and Wijffels, 2010) reported surface salinity increases in all oceans, especially at evaporation-dominated subtropical gyres. A more recent study (Aretxabaleta et al., 2017), also reports salinification of the Atlantic Ocean consistent with CC-induced changes in global hydrological cycle. Future SLR-scenarios for estuaries around the world include increases in estuarine salinity, estuarine water residence time, tide range, stratification, and tidal prism volume (Costa et al., 2023). The stability of shallow coastal ecosystems directly depends on the magnitude of CC and SLR (Timmerman et al., 2021).

SLR alters hydrologic gradients and pushes seawater further inland (Herbert et al., 2015) and, in some systems, will also result in higher salinity (Baldwin and Mendelssohn, 1998). CC is also forecast to increase temperature and evaporation and decrease freshwater inputs to coastal water bodies. As a result, strong salinification of the North Atlantic sub-tropical region is projected (Skliris, et al., 2020). Salinification of coastal waters will result in saltwater intrusion (Hong and Shen, 2012). Anthropogenic activities, such as over-pumping and paving urbanized areas are currently causing saltwater intrusion (Basack et al., 2022; White and Kaplan, 2017). SLR will aggravate the problem (Chang, 2011; Basack et al., 2022) by increasing hydrostatic pressure at the coast and favoring landward saltwater transport. Modeling coastal salinity regimes requires accurate representation of salinity fluctuations across ranges of the underlying physical drivers, as well as spatially across the landscape (Yurek et al., 2023). Robust and comprehensive models that represent coastal processes correctly are required for planning management scenarios. Models can provide valuable knowledge to decision makers by simulating alternative management practices that may improve both the productive and environmental values of coastal areas (Pavelic et al., 1997).

Reduction of the groundwater recharge zone due to land-use change, over-pumping, and SLR will produce landward hydraulic gradients (Jasechko et al., 2020). Large changes produced by CC are projected for the North Atlantic Ocean, including increased salinity near the southeast U.S. coast (Alexander et al., 2019). In six major estuaries along Florida's Gulf Coast, the extent, spatial orientation, and relative composition of coastal ecosystems may substantially change with SLR (Geselbracht et al., 2015). In coastal Florida all subsurface waters salinified between 1982–1987 and 2001–2015 (Szutz and Meinen, 2017). Local SLR may change coastal ecosystems by dry-land loss due to submergence and erosion, wetland loss and change, flood damage, saltwater intrusion, raising water tables, and impeding drainage (Geselbracht et al., 2015).

Near Miami, Florida, a shallow carbonate aquifer (Biscayne Bay) is an estuary that extends from the densely populated Miami metropolitan area (North Miami Beach) to the upper Florida Keys. Biscayne Bay counts with a comprehensive governance structure. At local scale, the Biscayne Bay Watershed Management Advisory Board (BBWMAB) advises the local government on various Biscayne Bay-related issues, provides local perspective, and makes recommendations for a new Miami-Dade County Biscayne Bay watershed management plan. In addition, the BBWMAB offers a local perspective on Biscayne Bay problems, issues, and solutions; and includes representatives from local government and a variety of local entities and groups, all of whom have demonstrated interest and commitment to Biscayne Bay matters (Miami-Dade County, 2021). At the regional level, the South Florida Water Management District (SFWMD) manages water resources of 16 Florida counties. These water governance boards, in conjunction with other national and regional institutions, identified significant CC impacts for the Southeast Florida region, including increasing average temperatures, more intense storm/drought events, and rising sea levels (Southeast Florida Regional Climate Change Compact Sea Level Rise Work Group, 2020).

Biscayne Bay has experienced seawater intrusion, likely exacerbated by the construction of leaky canals designed for drainage and flood protection (Jasechko et al., 2020). Salinity in the water column has also increased along the Biscayne Bay coast (SFWMD, 2020). In order to restore the quantity, quality, timing, and distribution of freshwater throughout the Everglades including estuaries, a number of initiatives are being implemented as part of the Comprehensive Everglades Restoration Plan (CERP). The Biscayne Bay Coastal Wetlands (BBCW) project is designed to rehydrate coastal wetlands in Biscayne Bay and reduce abrupt point source freshwater discharges that could be harmful to aquatic organisms (SFWMD, 2021). This will be accomplished through freshwater diversions with the goal of protecting and sustaining coastal resources for the future. Understanding the impact of freshwater delivery under SLR and CC is critical for developing freshwater management strategies across the flat, low-lying landscape of the coastal Everglades (Dessu et al, 2021).

In this research, a salinity transport model for Biscayne Bay is presented. The model is used to estimate spatial and temporal salinity distribution within the Bay for several scenarios. The scenarios were combinations of altered precipitation, increased salinity, increased temperature, and sea level-rise (SLR). The model is used to estimate spatial and temporal salinity distribution in the Bay. Based on the model predictions, we explore the potential implications on current restoration efforts of coastal Biscayne Bay and propose new management measures that could reinforce those efforts. Increased ocean salinity and temperature, and altered precipitation regime, are potential effects of CC. In this research, scenarios of altered precipitation, increased salinity, increased temperature are denominated as CC-induced scenarios.

2. Methods

2.1 Study area

Biscayne Bay is a lagoonal estuary located in southeast Florida. It covers approximately 700 km^2 with an average depth of 2 m, although the northern Bay has sections with depths ranging up to 15 m (**Figure 1**). The area surrounding the Bay, which was once dedicated to agriculture, has experienced rapid urban growth in the last decades (Millette et al. 2019).

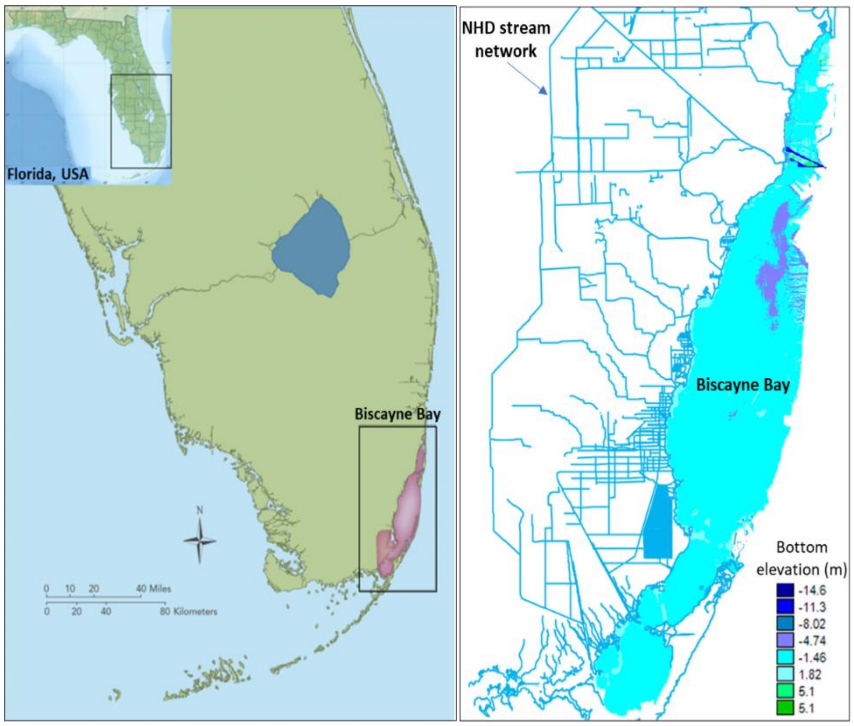

Figure 1. Biscayne Bay and surrounding canals and streams as represented by the US National Hydrography Dataset (NHD).

The climate in south Florida is subtropical, 60% of the annual rain falls during the wet summer months of May to October. Annual precipitation ranges between 1000 mm to 1800 mm. The month with the most wet days is August, with an average of 18.8 days with at least 1 mm of precipitation. The drier season lasts approximately 7 months, from late October to mid-May. The month with the fewest wet days is January. Monthly probability distributions of climate change in South Florida predict that by the year 2060 precipitation will increase or decrease by 10 % (Nungesser et al., 2015).

Twelve canals discharge into the bay. The total discharge volume averages 56 m^3/s, with 70% to 90% of that flow occurring during the wet season (Alarcon et al., 2022a; Stabenau et al., 2015). The average hourly wind speed in Biscayne Bay varies seasonally. The windier part of the year is from October to May, with average wind speeds of more than 4.8 m/s (Alarcon et al., 2022a). The windiest month of the year is November, with an average hourly wind speed of 5.8 m/s. The predominant wind direction is from the east.

Watersheds draining to the Bay have a complex water management system composed of levees, reservoirs, and canals along with their water control structures (Wilsnack et al., 2019). This water management system serves to drain historical wetlands and provide flood protection to human populations. Managers in the region regulate water depths in the extensive canal network to control groundwater levels and reduce saltwater intrusion into the underlying karst aquifer (Czajkowski et al., 2018). Figure 1 shows the US National Hydrography Dataset (NHD) stream and canal network feeding into the Bay.

2.2 Salinity model

Hydrodynamic modeling of the bay (described in Alarcon et al., 2022a) used hourly data for water surface elevation (WSE), air temperature, wind speed, and wind direction available at NOAA's Virginia Key Station (NOAA, 2020). River stage data for main streams draining to Biscayne Bay (canals, creeks, etc.) were obtained from the SFWMD's DBHYDRO platform (SFWMD, 2020), and used to calibrate and validate the hydrodynamic model. Stream flows from main tributaries to the Bay (**Figure 2A**) were also obtained from SFWMD (2020). Wind and temperature data were obtained from the NOAA Virginia Key Station (Alarcon et al., 2022a). The EFDC+ software (DSI, 2017) was used for simulating the hydrodynamic regime in the Bay. The governing equations of EFDC+ include Navier-Stokes for fluid flow, the advection-diffusion equations for salinity, temperature, dye, toxicants, eutrophication constituents and suspended sediment transport. In the horizontal direction, the equations are presented in the curvilinear coordinate system, discretized with the finite difference method based on an explicit scheme (DSI, 2017). EFDC+ takes account for e Coriolis and curvature accelerations.

The estimation of the salinity regime in Biscayne Bay was based on an existing validated hydrodynamic model (described in Alarcon et al., 2022a). The existing hydrodynamic model (Figure 2A) consists of 9,434 grid cells, two vertical layers, nine freshwater input cells (main streams draining to Biscayne Bay), and three open-ocean boundaries that represent the connection of the Bay with the Atlantic Ocean. For fast convergence and enhanced stability, the Bay was represented by rectangular cells. The following variables were iteratively changed to generate an efficient computational representation of the water body: computational grid spatial resolution, location of boundary conditions, curvilinear versus cartesian coordinates, and numerical criteria (time-step, numerical algorithm, etc.) (Alarcon et al., 2022a). To implement salinity transport, salinity boundary conditions were set up at the ocean water entrance to the estuary (**Figure 2B**). Three-dimensional salinity transport was calculated using the salinity module available in EFDC+. The governing equations include the Navier-Stokes equations for fluid flow (Boussinesq approximation for variable density modeling in the momentum and continuity equations), and the transport equations for salinity and temperature.

Groundwater flows were estimated using the United States Geological Service's Modular Three-dimensional Finite-difference Groundwater Flow Model (MODFLOW). The model, described in Alarcon et al. (2022b), was set up to calculate groundwater flows along the Biscayne Bay coast. Groundwater time-series calculated by MODFLOW were input to the hydrodynamic model as external forcing data.

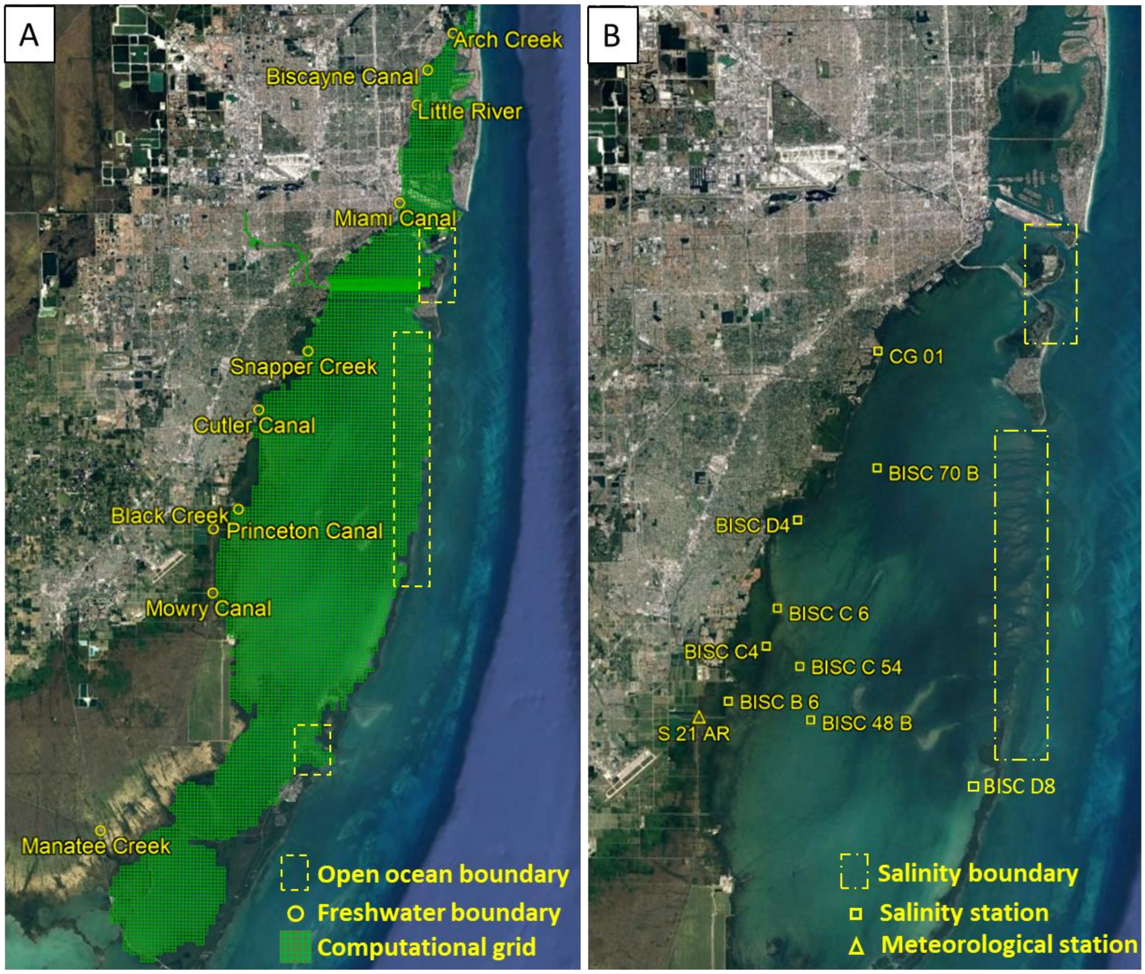

Figure 2. Freshwater and ocean inflows, salinity stations, and a meteorological station in Biscayne Bay are depicted. A) Hydrodynamic model grid of Biscayne Bay, freshwater and ocean boundaries. B) Salinity stations, salinity ocean boundaries (BISC D8), and meteorological station at Biscayne Bay (S21 AR).

2.3 Observed salinity in Biscayne Bay

Coastal drainage canals and natural streams, precipitation, and groundwater feed freshwater to Biscayne Bay (Stalker et al. 2009). The variability in freshwater inputs creates unique salinity distributions across Biscayne Bay (Alarcon et al., 2022b). Salinity data from the following monitoring stations are used to characterize the salinity regime in the Bay: CG 01, BISC 70 B, BISC D4, BISC C6, BISC C4, BISC C6, BISC B6, BISC 54B, BISC 48B, and BISC D8 (Figure 2B). The data was obtained through the DBhydro environmental database (SFWMD, 2020).

2.3.1 Analysis of observed salinity in Biscayne Bay

Salinity data from three stations are used to illustrate the different temporal and spatial distribution of salinity in Biscayne Bay (**Figure 3**). The stations were chosen to show the wide range of observed salinities depending on geographical location. Drastic changes in salinity (from less than 5 PSU to greater than 40 PSU) at central coastal locations (BISCD4), less extreme salinity range

(20 PSU to 38 PSU) at Coral Gables Canal outfall (CG 01) in the North, and typical ocean salinity ate the ocean boundary (BISCD8).

Figure 3 also shows the salinity relationship to precipitation. Precipitation data corresponds to Station S21AR (closest meteorological station to Central Biscayne Bay). In general, salinity decreases with greater precipitation volumes during the wet season (May to November) and increases during the dry season (December to April). Minimum salinity values occur during months where the highest monthly precipitation peaks were observed (years 2017, 2018, and 2019) or after sustained monthly precipitation during the wet season (years 2012 to 2016). March is the driest month during the 2012-2019 period, and November marks the end of the wet season. However, observed salinity minimums and maximums do not coincide with those months. This delay in salinity minimums and maximums has also been reported in adjacent Florida Bay (Kelble et al. 2007). Although the years 2015 and 2016 had similar annual precipitation volumes (1450 and 1420 mm, respectively), observed maximum and mean salinities in 2015 are noticeably higher than in 2016. Salinities in the year 2016 are consistently less than 33 PSU and greater than 15 PSU, being the year with the most uniform temporal distribution of salinities.

The years 2015 and 2016 capture the diversity of the salinity regime observed from 2012 through 2019. Salinity in mid-2015 reached more than 42 PSU (11 PSU above 2015 annual salinity average), and by the end of 2015 observed salinity was approximately 13 PSU (18 PSU lower than the 2015 average). During 2016, the temporal distribution of salinity was much more even around the annual mean (25.8 PSU). This average value was about 20% less than the 2015 mean annual salinity (31.1 PSU). Therefore, in this research, years 2015 and 2016 were selected as base-case scenarios for model evaluation. Focusing on specific annual events to understand the salinity dynamics at coastal waters is common in recent research (Poppeschi et al., 2021; Du and Park, 2019.

The freshwater volume that drains to the bay through the natural and man-made streams is less than 1% of saltwater volume that enters the bay through the ocean boundary (Alarcon et al., 2022a). Therefore, ocean salinity drives the salinity regime in Biscayne Bay (Wang et al., 2003). The episodic dilution of salinity at the coast occurs due to delayed arrival of fresh groundwater flows. The groundwater model for the area (Alarcon et al., 2022b) predicted that it would take 4 to 7 days for groundwater to travel from the recharge zone to the coast. Extreme salinity peaks occur during drought periods where less surface and groundwater flow occurs. Increases in salinity at the coast may be due to reflux of intruded salty water during low tide (Prinos, 2016) and also residence times ranging between 15 days to a month (Alarcon et al., 2022; Wang and Luo, 2003).

2.4 Model calibration and validation

Calibration and validation of the hydrodynamic model was performed comparing predicted hourly water surface elevations (WSE) to observed data at several locations inside Biscayne Bay and the Coral Gables Canal. Alarcon et al. (2022a) shows the robustness of the hydrodynamic model by simulating successfully hourly mean WSE and also extreme WSE (Irma Hurricane).

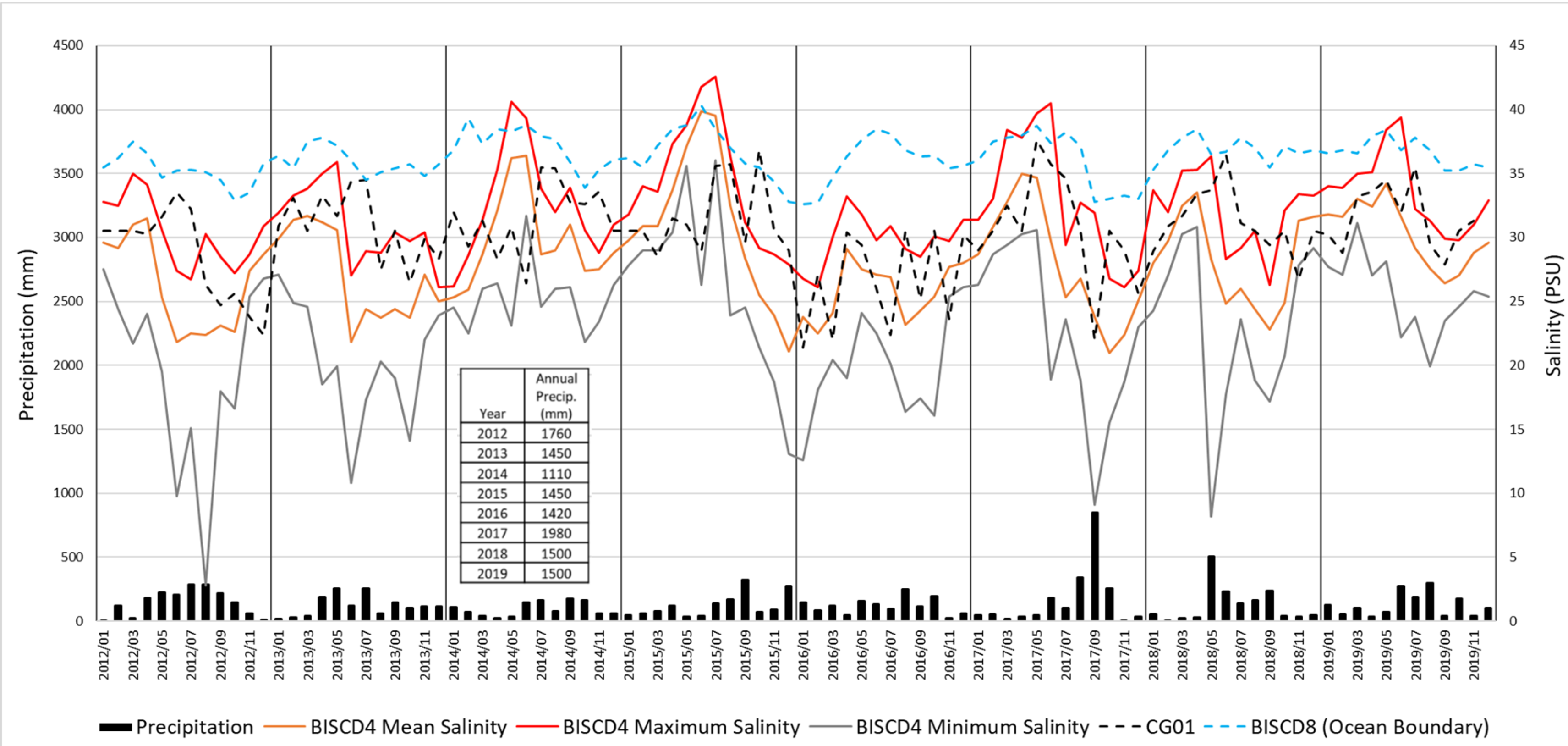

Figure 3. Monthly precipitation and salinity (mean, maximum and minimum) at central Biscayne Bay (BISCD4 salinity station). Stations BISCD8 and CG01 are also show.

Salinity calibration was performed through a heuristic process. Simulation of offshore salinity did not require significant adjustments of default model parameters because offshore salinity is strongly dependent on salinity at the ocean boundary. Since hydrodynamic transport was successful, salinity transport from the ocean boundary to offshore locations was optimal. Salinity near the coast, however, is influenced by freshwater inflows. A MODFLOW groundwater model (described in Alarcon et al., 2022b) was developed to account for groundwater inflows to the Bay. The position and extent of the groundwater recharge zone of the groundwater model) were used as main calibration factors of coastal salinity modeling. Groundwater recharge was calculated from precipitation and evapotranspiration data collected at weather stations in the area.

The strategy for calibrating and validating simulated outputs consisted of achieving acceptable salinity estimations of hourly offshore and coastal locations during calibration, and then validating monthly model outputs at coastal locations. Salinity calibration was performed comparing hourly observed and simulated salinity for stations CG01, BISC70B, BISCD4, BISCC6, BISC54B, BISCB6, BISCC4, BISC48B (years 2012 to 2014). The validation phase was performed comparing monthly observed and simulated salinity at stations BISCC4, BISC70B, BISCC6, BISCD6, and BISCD4 (years 2012 to 2019). Goodness-of-fit statistical indicators for assessing the quality of model simulations are summarized in Table 1, including acceptability ranges for hourly and monthly simulations. The acceptability range for the Kling-Gupta indicator (K-G) shown in Table 1 is suggested by Knoben et al. (2019). The ranges of acceptability for R^2, d, PBIAS are suggested by Moriasi et al. (2007). In general, acceptability ranges for greater time-steps are more stringent than for shorter time steps (Moriasi et al., 2007).

Table 1. Statistical indicators of goodness-of-fit and corresponding acceptability ranges.

Indicators of Fit	**Formulae**	**Range (monthly simulation)**	**Range (hourly simulation)**
Percent bias, *PBIAS*	$\frac{\sum_{i=1}^{n} \left(Y_i^{Obs} - Y_i^{Sim}\right) * 100}{\sum_{i=1}^{n} (Y_i^{Obs}).}$	<±18%	<±25%
Correlation coefficient, *R*	$\sqrt{\frac{\sum_{i=1}^{n} (Y_i^{Sim} - Y_i^{Mean}).^2}{\sum_{i=1}^{n} (Y_i^{Obs} - Y_i^{Mean}).^2}}$	> 0.85	>0.71
Coefficient of determination	R^2	> 0.6	> 0.5
Kling-Gupta efficiency, *K-G*	$1 - \sqrt{\left(\frac{Y_{Sim}^{Mean}}{Y_{Obs}^{Mean}} - 1\right)^2 + \left(\frac{STDEV_{Sim}}{STDEV_{Obs}} - 1\right)^2 + (R-1)^2}$	> 0.6	> 0.50
Willmott's index of agreement, *d*	$1 - \frac{\sum_{i=1}^{n} \left(Y_i^{Obs} - Y_i^{Sim}\right).^2}{\sum_{i=1}^{n} \left(\lvert Y_i^{Sim} - Y_{Obs}^{Mean}\rvert + \lvert Y_i^{Obs} - Y_{Obs}^{Mean}\rvert\right).^2}$	> 0.66	> 0.55
$Y_i^{Obs} = Observed\ salinity\ concentration$ $Y_i^{Sim} = Simulated\ salinity\ concentration$ $Y_{Obs}^{Mean} = Mean\ of\ observed\ salinity\ concentration$ $Y_{Sim}^{Mean} = Mean\ of\ simulated\ salinity\ concentration,$ $n = Total\ number\ of\ hourly\ salinity\ concentrations$			

2.5 Simulation scenarios and salinity restoration

Restoration plans, including CERP, generally assume a stable climate, yet projections of altered climate over a 50-year time horizon suggest that this assumption may be incorrect. Nungesser et al (2015) estimated a temperature rise of 1.5 C, a ±10 % change in rainfall, and a 0.46 m SLR relative to base conditions in the study region by mid-21st century. Alarcon et al. (2022a) estimated SLR ranging from 0.63 m (by 2160) to 2.18 m by 2120 (NOAA Intermediate Scenario). Skliris et al. (2020) and Bindoff et al. (2019) project increases in salinity in the upper layer (0 – 500 m) for the North and South Atlantic oceans under both RCP4.5 and RCP8.5. Silvy et al. (2020), through the Coupled Model Intercomparison Project 5 (CMIP5) for RCP 8.5, estimates that salinity at the end of the twenty-first century will increase by 0.60 Practical Salinity Unit (PSU) at the Biscayne Bay ocean boundary.

In this research, the combined CC-induced and SLR scenarios detailed in Table 2, are simulated using the calibrated and validated salinity model. These scenarios assume: (1) a constant increase in temperature of +1.5°C; (2) a constant increase in salinity at the ocean boundary of +0.6 PSU; (3) variable changes in precipitation of ±10% in the rainy and dry seasons, and varying increases in SLR of +0.46, +1.72, and +2.18 m. In total, nine CC-induced and SLR scenarios were simulated. These scenarios were chosen based on the NOAA Intermediate-High SLR projections for years 2050, 2100, 2120. Two baseline years (2015 to represent high salinity and 2016 to represent low salinity). Three representative months March (end of the dry season), July (middle of the rainy season, and November (end of the rainy season) were chosen for simulate salinity changes in Biscayne Bay under the proposed scenarios.

Table 2. Combined CC-induced and SLR scenarios.

Sea level rise (m)	Precipitation (% increase)	Temperature (°C)	Salinity increase at the ocean boundary (PSU)
+0.46	+10	+1.5	+0.6
+0.46	-10		
+0.46	+10 (rainy season) -10 (dry season)		
+1.72	+10		
+1.72	-10		
+1.72	+10 (rainy season) -10 (dry season)		
+2.18	+10		
+2.18	-10		
+2.18	+10 (rainy season) -10 (dry season)		

The predicted scenarios were analyzed to determine which combination of CC-induced and SLR impacts produced the highest increase in bay salinity (worst-case), and which combination produced the lowest increase in salinity (mildest scenario). For each of those scenarios, an estimation of the quantity of freshwater inputs required to counterbalance the salinity increase was performed, i.e., increases in freshwater flows to restore the scenario salinity to current salinity conditions were calculated.

3. Results

3.1 Comparison of observed and simulated data during calibration and validation

The comparison of observed and simulated data during model calibration (Annex A, Table A1, Figure A1) shows that the model reproduces the wide shifts in salinity observed at coastal salinity stations. The coefficient of determination (R^2) values for offshore stations BISC70B, BISC 54B, and BISC48B) are within acceptability range ($R^2 > 0.5$). For coastal stations, simulated output exceeded acceptability thresholds at all stations for the Kling-Gupta Efficiency and Percent Bias. Indices of agreement for all stations except BISC48B comply with the acceptability range. Also, the model captures trends and rapid shift of salinity values observed in coastal stations BISCC4, BISCB6, BISCC6, and BISCD4. Most of the rehydration efforts are concentrated along the central coast of Biscayne Bay where those stations are located (SWMD, 2021).

The model validation phase was based on monthly comparison of observed and simulated salinity for years 2012 to 2019 (**Figure 4**, **Table 3**). Figure 4 shows observed and simulated salinity time-series at coastal observational stations. The comparison demonstrates that monthly simulations reproduce optimally the monthly salinity regime in Biscayne Bay. Model predictions at all coastal stations exceed the statistical acceptability thresholds for all goodness-of-fit indicators (Table 3). Therefore, the calibrated and validated salinity model can now be used to explore salinity under different CC-induced and SLR scenarios.

3.2 Spatial distribution of salinity

3.2.1 *Relative change in salinity spatial distribution for baseline year 2015*

The simulated spatial distribution of salinity for all scenarios predicts at least 10% salinity increase along the central coast of Biscayne Bay (**Figure 5**). In relation to observed salinities, this means that at the end of the dry season (March) salinities would reach at least 34 PSU, during the middle of the rainy season (July) salinities could reach 46 PSU, and after the rainy season (November) salinities would approximately be 25 PSU. In all simulated scenarios, a sustained salinity increase at the central coast of Biscayne Bay is predicted, this increase spreads towards mid bay especially at the end of the dry and the end of the rainy seasons.

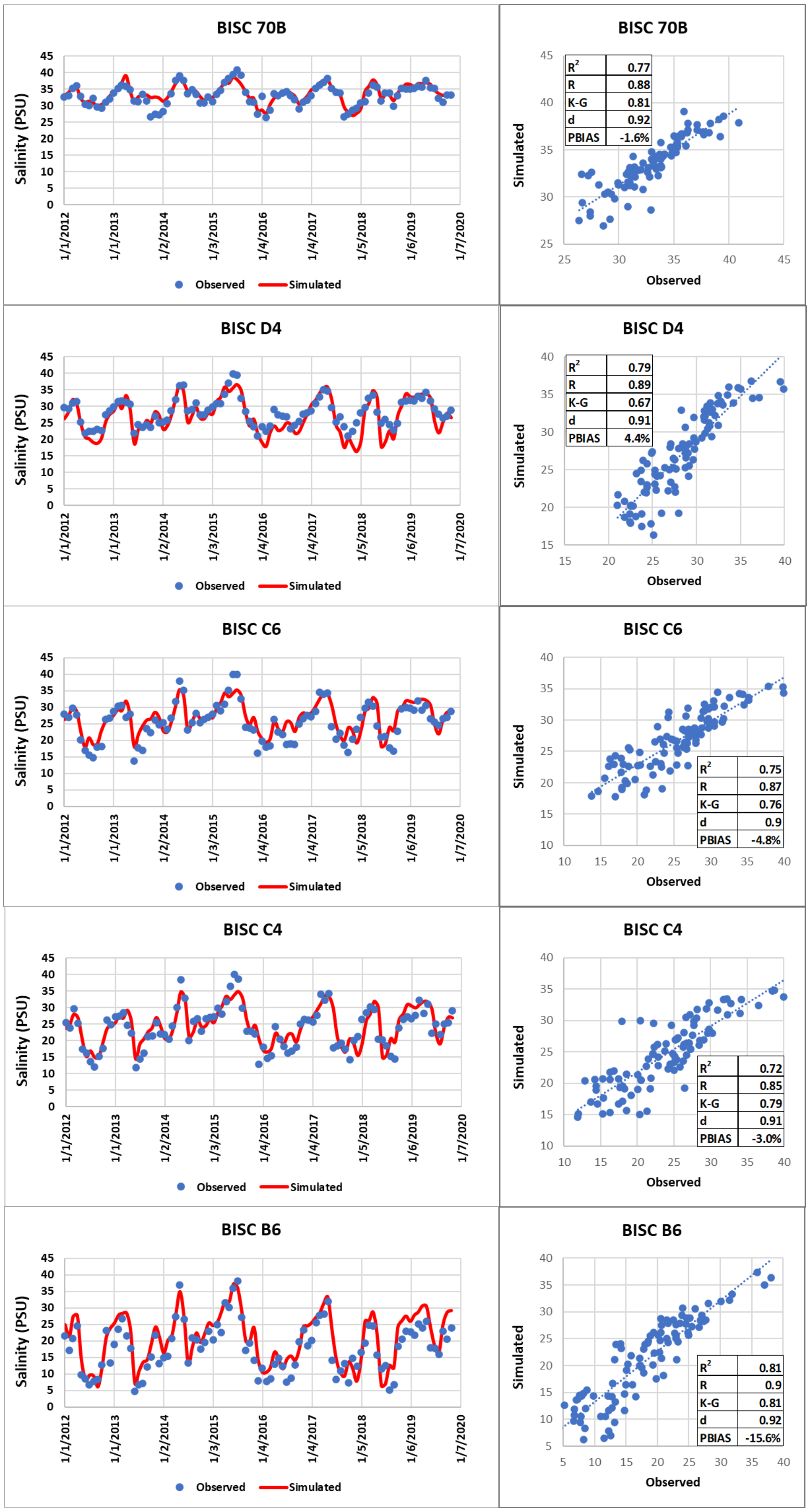

Figure 4. Validation of the salinity model. Observed and simulated salinity time-series and scatter plots are shown for coastal stations.

Table 3. Statistical fit of simulated salinities during validation.

Station	Indicators of fit				
	$R^2 > 0.6$	R > 0.85	KG > 0.6	Index of agreement, d> 0.66	PBIAS < ±20%
BISC70B	0.77	0.88	0.81	0.92	-1.6%
BISCD4	0.79	0.89	0.67	0.91	4.4%
BISCC6	0.75	0.87	0.76	0.90	-4.8%
BISCC4	0.72	0.85	0.79	0.91	-3.0%
BISCB6	0.81	0.90	0.81	0.92	-15.6%

Although precipitation in July (mid wet season) was not the highest during the baseline-year 2015, the model predicts that even with a future decrease of 10% in precipitation, and an increase in 0.6 PSU of salinity at the ocean boundary, the percent increase in salinity in July would be more moderate than at the end of the dry season (March) or the end of the wet season (November). Therefore, even moderate inputs of freshwater into the system would contribute to decrease salinity concentrations under extreme conditions (mid wet season). This is consistent with observed salinities at the coast (Figure 3). Moderate rain events at the end of year 2013 and beginning of year 2014 (driest year) decrease salinity peaks in July. The largest increases in salinity for baseline year 2015 under all CC-induced scenarios occurred near the shore of central Biscayne Bay. The largest decreases in salinity were in southern Biscayne Bay.

The model suggests that the impact of SLR in salinity spatial distribution is somewhat proportional to the magnitude of the rise. SLR magnitudes used in this research increase the flux area available at the ocean boundary. Therefore, the amount of ocean water that enters Biscayne Bay through the ocean boundary will increase (with respect to current conditions) during high tide. Consequently, salinity in the bay will increase with SLR regardless of inland freshwater inflows, since those are comparatively much smaller than ocean inflows. Also, residence times at the coast (15 days to 1 month) allow salinity concentration to increase.

In relative terms, the scenario corresponding to 1.5°C increase in temperature, a 10% decrease in precipitation, 2.18 m SLR, and 0.6 m increase in ocean salinity, produces a sustained spatial increase in salinity throughout Biscayne Bay (worst-case). The mildest CC scenario was identified under 1.5 °C increase in temperature, a 10% increase in precipitation, 0.46 m SLR, and a 0.6 PSU increase in ocean salinity.

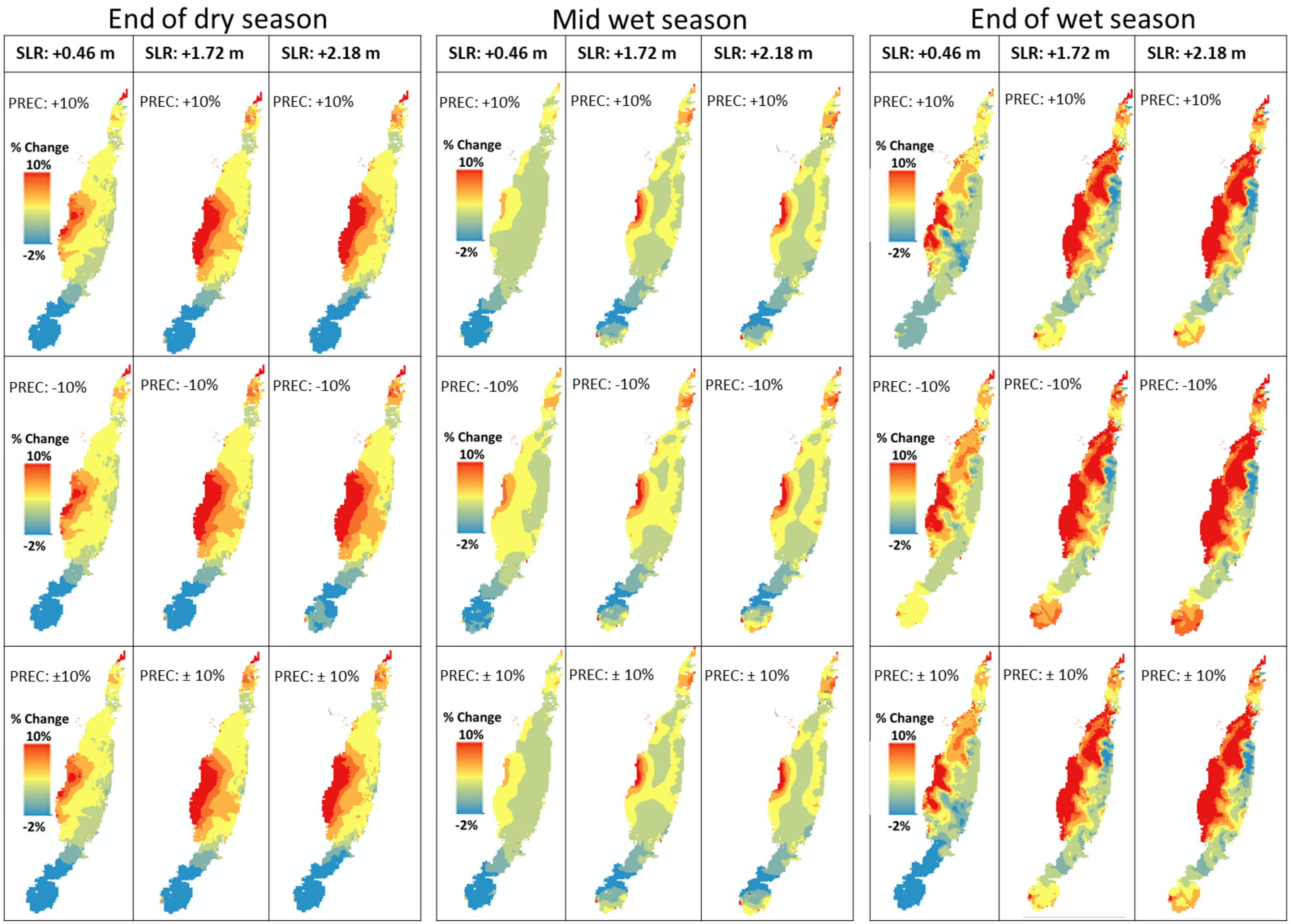

Figure 5. Relative change in salinity under climate change scenarios for baseline year 2015. Simulations include an increase in ambient temperature of +1.5°C and an increase in ocean salinity of +0.6 PSU.

3.2.2 *Relative change in salinity spatial distribution for baseline year 2016*

The changes relative to baseline year 2016 were more pronounced with a larger portion of the bay having salinity increases greater than 10% (**Figure 6**). The model indicates that a less salinified Biscayne Bay in 2016 would be relatively more sensitive to increased ocean salinity and SLR. The simulations show that relative increases in salinity are greater in spatial extent than those calculated for baseline year 2015. The simulated spatial distribution of salinity for all the CC scenarios predicts at least a 10% salinity increase along the central coast of Biscayne Bay, and comparative increases in the northern and southern bay regions as well. As in 2015, the hydrodynamic regime in 2016 pushes salt water towards the central coast and northern Biscayne Bay.

The model predicts that salinities in November will not increase as much as during March and July for baseline year 2016, even though salinities were slightly higher in the base case. This results from the cumulative effect of sustained moderate precipitation events during the rainy season. Again, the rationale for the beneficial effects of constant and moderate freshwater inflows to keep salinities low is evident.

As in baseline year 2015, the model-predicted worst-case scenario for baseline year 2016 corresponds to a 1.5°C increase in temperature, a 10% decrease in precipitation, 2.18 m SLR, and 0.6 m increase in ocean salinity. The mildest increase in salinity was predicted to occur for a 1.5°C increase in temperature, a +10% change in precipitation, 0.46 m SLR, and 0.6 m increase in ocean salinity (mildest-case scenario). From visual inspection of Figures 5 and 6, an intermediate scenario would correspond to 1.5°C increase in temperature, ±10% change in precipitation, 0.46 m SLR, and 0.6 m increase in ocean salinity.

Figure 7 shows monthly averaged salinity distribution in Biscayne Bay for the three scenarios identified as mildest, intermediate, and worst, for baseline year 2016. The figure shows that salinity in March (under all scenarios) ranges from 28 PSU up to 35 PSU. In July, most of Biscayne Bay is estimated to have salinities greater than 37 PSU, reaching 42 PSU for at least half of the Bay area.

The model predicts that at end of the rainy season (November) bay salinity decreases in all scenarios with respect to March and July salinities. Freshwater inputs coming from Snapper Creek and Black Creek refresh coastal regions in central Biscayne Bay. Arch Creek, Biscayne Canal, Miami River, and Little River cause the same effect in Northern Biscayne Bay.

3.3 Freshwater inputs required to return to current salinity conditions

Section 3.1 established that altered temperature, precipitation, salinity, and SLR, will increase salinity throughout Biscayne Bay even in the mildest scenario. In this section we estimate the quantity of freshwater inputs required to counterbalance the salinity increase, i.e., the proportion in which freshwater flows should be increased to restore increased salinities to current salinity conditions.

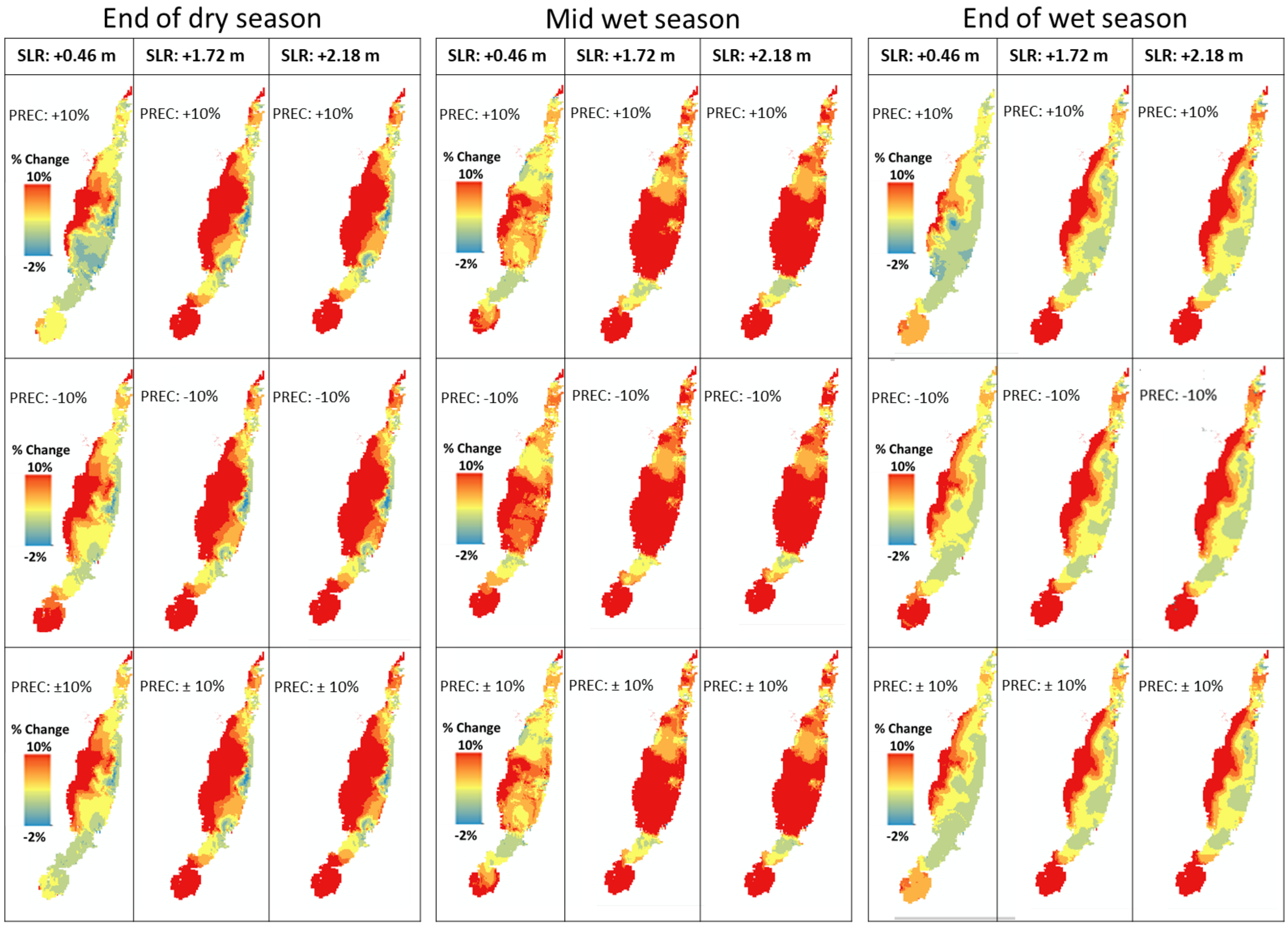

Figure 6. Relative change in salinity under CC-induced and SLR scenarios for baseline year 2016. Simulations include an increase in ambient temperature of +1.5°C and an increase in ocean salinity of +0.6 PSU.

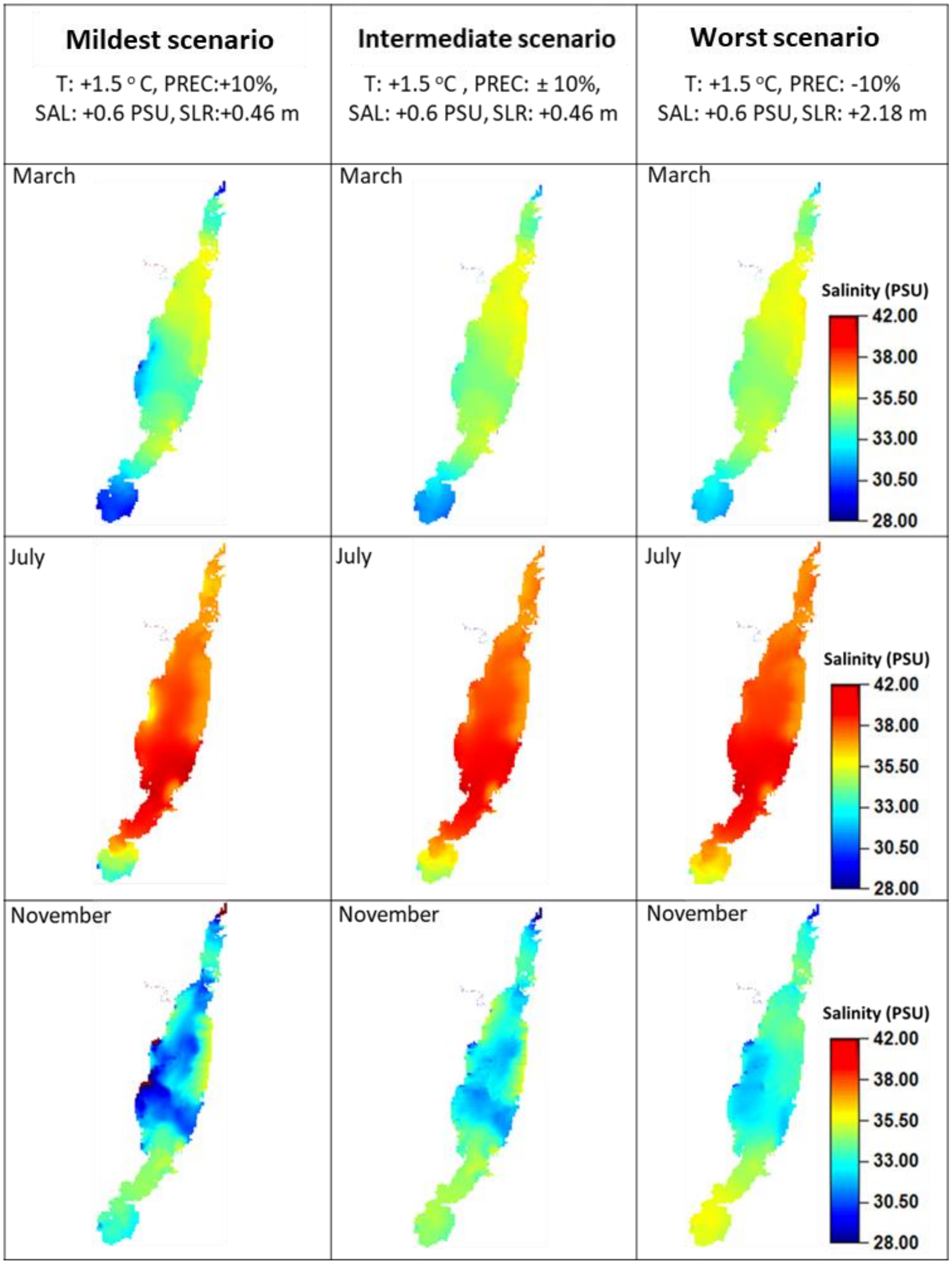

Figure 7. Spatial distribution of salinity under CC-induced and SLR scenarios.

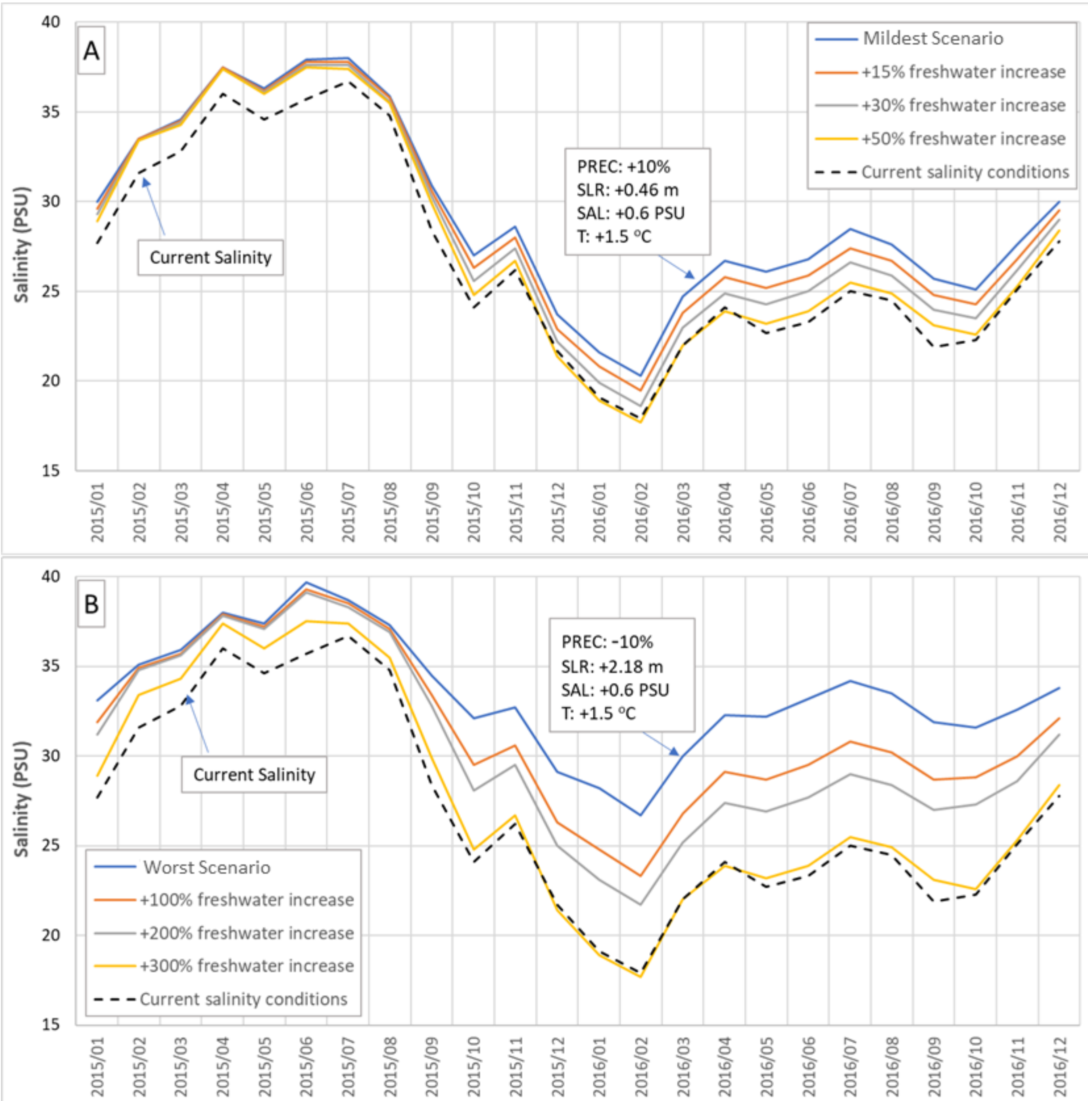

Figure 8. Freshwater inputs required to return to current salinity conditions. A) Mildest scenario. B) Worst scenario.

Salinity concentrations at station BISCD4 were calculated for baseline years 2015 and 2016 (baseline years) under the following scenarios (**Figure 8**):

- Current conditions: salinity regime observed during 2015 and 2016, freshwater inputs observed during those years (baseline precipitation, and temperature).
- Mildest scenario: precipitation (PREC) increased in +10%, +0.46 m SLR, salinity at the boundary (SAL) increased in 0.6 PSU, temperature (T) increased in +1.5°C.
- Mildest scenario with baseline freshwater inputs increased by 15%, 30%, and 50%.
- Worst scenario: PREC decreased -10%, +2.18 m SLR, SAL increased in 0.6 PSU, and T increased in +1.5°C.
- Worst scenario with baseline freshwater inputs increased by 100%, 2000%, and 300%.

For the mildest scenario (Figure 8A), increasing the freshwater inflows by 15%, 30%, or 50% would have minimal effects during an extreme dry season as observed in early 2015. However, from August 2015 to the end to 2016, the model estimates that a 50%-increase in baseline freshwater inputs would lower the salinities corresponding to the mildest scenario to observed salinities in the baseline years (current conditions). Moreover, both the 15% and 30% increases in freshwater decrease salinity in the bay, but do not restore the salinity to the current salinity conditions. For the worst scenario, a 300%-increase of baseline freshwater inputs was required to decrease the scenario salinity to current conditions (Figure 8B).

3.4 Discussion

This research shows that efforts aimed to restore salinity to “natural” conditions in Biscayne Bay are challenged by increased coastal water salinification under any simulated scenario. Nevertheless, analysis of historic precipitation data for 2016 shows that modest freshwater inflows evenly distributed throughout the year, generated a moderate salinity range (15 PSU to 35 PSU) at the coast. Management measures that would generate modest steady increases in freshwater inflows may have similar effects under current and future scenarios.

3.4.1 *Management measures*

Local hydrological processes can be managed to reduce evapotranspiration and promote infiltration and aquifer recharge. Current increase of salinity at the Biscayne Bay coast responds to unbalanced arrival of freshwater flows to the coast. Rapid runoff, decreased infiltration, and high evaporation do not promote groundwater recharge and flow.

Urban greening (UG) is a management practice that involves organized or semi-organized efforts to introduce, conserve, and maintain outdoor vegetation in urban areas (Smart et al., 2020). UG mitigates the disturbance of natural drainage in cities by promoting rainfall interception, gradual release of rainwater to the ground, and storage of rainwater in branches and leaves (Alarcon and Callejas, 2023; Derkzen et al., 2015). Incorporating street trees into urban landscapes can reduce runoff by 62%, being this reduction largely attributed to infiltration into the tree pit (Berland et al., 2017). Urban forests have temperatures that are lower than in unforested urban areas (Knight et al., 2021). A reduction in temperature would decrease evaporation losses. If UG is implemented at parcel scale, deep drainage is increased by 100% within urban parcels (Voter and Loheide, 2018). The benefits of urban greening for water management under CC-impacts has been demonstrated in Europe extensively (Quaranta et al., 2021; Pauleit et al., 2019). UG is feasible to be implemented in urban areas surrounding Biscayne Bay. A recent quantification of urban vegetation in the Miami-Dade area (Hochmair and Benjamin, 2021) revealed that 60 percent of the municipalities have lower that 20% urban tree canopy with large portion of the area offering potential for increasing urban tree canopy in at least 15%. In the United States, urban tree cover averages 39.6% (Nowak et al., 2022). Conservatively, we assume that UG implementation would generate 40% additional freshwater inputs to Biscayne Bay through enhanced infiltration, and evaporation reduction.

Artificial groundwater recharge with treated wastewater is a sustainable management measure to preserve the groundwater water table, and restore water resources in aquifers (Shawaqfah et al., 2021). Treated wastewater typically provides the steadiest freshwater supply for aquifer recharge, and the least competition from other water users (Luxem, 2017). Groundwater recharge with treated wastewater is not new in the USA. In 1976, a 67000 L/s facility began recharging treated wastewater to a California aquifer (National Research Council, 2008). In Florida, a man-made aquifer storage recovery system is in operation since 1992 (Reese, 2002). The system was constructed to recharge into the Hawthorn formation, which is located within the upper Floridan Aquifer, underlaid by karst terrain. Therefore, a similar aquifer recharge system can be built to recharge the Biscayne aquifer. However, migration from the current septic system to sewer system is necessary for implementing aquifer recharge using treated wastewater.

The water supply source in the Biscayne Bay area is the Biscayne aquifer. Saltwater intrusion is exacerbated by freshwater pumping from the aquifer for urban consumption. The largest water consumption in the Miami-Dade area is residential (Miami Dade Government, 2007). The per capita consumption of water in 2009 was 527 liters of water per day. Although water consumption reductions are planned (e.g., 20% reduction by 2025 in Coral Gables, Florida), additional reductions are necessary. For example, the average per capita consumption in Europe is 144 liters per day. Decreasing freshwater consumption will reduce over exploitation of the aquifer, promote additional groundwater volumes to flow to the Biscayne Bay coast, and reduce saltwater intrusion.

Miami-Dade has 2.6 million inhabitants. If per capita water consumption is reduced to 300 liters per day, approximately 9 m^3/s of treated domestic wastewater could be used for year-round aquifer recharge. Similarly, a per capita reduction of 200 liters per day in water consumption could generate 6 m^3/s of additional groundwater flow. Aquifer recharge with treated wastewater and water consumption reduction could add 15 m^3/s to current 56 m^3/s total canal discharge. Adding UG-generated freshwater, totals approximately 55% increase in freshwater inputs to the bay, which is sufficient to mitigate the mildest salinification scenario.

3.4.2 *Application to other locations*

The results of this research may be applicable to urbanized coastal areas located in the subtropical gyre, which have access to important freshwater resources, and are underlaid by highly porous and/or fractured aquifers (not necessarily karst). In the world, 15.7% of marine coastlines are characterized by carbonate rocks, and 13.1% occur in tropical climates where important groundwater recharge is provided during the rainy season (Goldscheider et al., 2020). Estuaries and coastal regions with similar environmental forcings and governance levels to Biscayne Bay may transfer the proposed management approach easily. Nevertheless, the applicability of similar management practices in locations with lower degrees of water governance would not be straightforward.

Merida is the largest city in southeastern Mexico (600,000 inhabitants), located in the Yucatan State, on the Gulf of Mexico coast. The region has an average annual rainfall between 500 and 1500 mm, most of it being restricted to the rainy period (Escolero et al., 2000). Yucatan's climate has been getting hotter (Sastaretsi-Sioui, 2019), and SLR is likely to reach 0.67 m to 2.23 m in this century (Boretti, 2019). Coastal waters in the Yucatan peninsula are also becoming saltier (Wu et al., 2017). The city and industrial and agricultural sectors obtain its freshwater from a karst aquifer (Escolero et al., 2000). Mexico invested only 2.82% of GDP into infrastructure (one of the lowest percentages in Latin America and Caribbean) from which only 0.08% corresponded to water infrastructure investments (Moran-Valencia et al., 2023). Nevertheless, the Yucatan State water management structure is rated as having very high efficiency but lacking initiative for improvements of the water system (Moran-Valencia et al., 2023). Yucatan State seem to have governance structures and technical know-how to implement the management measures suggested in this research, but the federal and local governments need to have the political will to invest a higher percentage of GDP into water infrastructure.

Lagos City in Nigeria is underlain by the Benin Basin that consists of several aquifers composed by sands and shales, with some limestone which thicken towards the west and the coast as well as down dips to the coast (Oladapo et al., 2014). Freshwater is extracted from those aquifers through hand-dug wells and boreholes. Groundwater is adequately recharged (mean annual rainfall is 2000 mm) (Yusuf and Abiye, 2019). Saltwater intrusion in the aquifers has been identified (Aladejana et al., 2020) mainly due to excessive exploitation of groundwater (Yusuf and Abiye, 2019). Increasing temperatures have been observed (Elias and Omojola, 2015). Since Nigeria's coastal areas are within the subtropical gyre, salinification of coastal waters is likely. Natural resources in Nigeria are owned by the government but the exploitation of water resources was deregulated with the aim of enhancing access to water supply as a human right. Nevertheless, the deregulation was not equipped with a water policy (Ukpai, 2022). Clearly, water governance is underdeveloped. Before attempting management measures in the city and region, existing water governance structures should be reinforced with cross-sectoral engagement. This will place trust among the public and competing stakeholders for adequate water resources exploitation and restoration.

3.4.3 *Social and ecological effects*

Biscayne Bay is the main environmental feature in Miami Dade county. Activities such as bay-related recreation, commercial and recreational fishing, Port of Miami, shipping, and marine-related industries depend on the water quality of the bay. The Bay houses a variety of ecologically and commercially important coastal and marine species that depend on specific salinity regimes.

The juvenile and adult marine species that are currently imperiled are the Florida manatee (*Trichechus manatus latirostris*), the smalltooth sawfish (*Pristis pectinata*), the American crocodile (*Crocodylus acutus*), and Johnson's seagrass (*Halophila johnsonii*). Manatees are mammals and need fresh water to drink. High levels of salinity affect manatee movement patterns (Butler and Reid, 2004). Smalltooth sawfish is a euryhaline species that thrive in salinities between 21.4 and 34.7 PSU (Simpfendorfer, 2001). Young crocodiles are particularly sensitive to high salinity, and they need nursery habitat with low salinity around nesting sites (Harvey et al., 2016). Johnson Grass growth and survival are significantly affected by salinity. Maximum growth and survival rates were observed at 30 PSU (NOAA, 2007).

Commercial and recreational fishing may be the most sectors affected by changes in the salinity regime. The most valuable Biscayne Bay species for fishery are pink shrimp (*Penaeus duorarum*) and spiny lobster (*Panulirus ornatus*). For P. Ornatus, growth is highest at 35 PSU and progressively less at lower salinities. (Jones, 2009). Pink shrimp growth is optimal in the mid-range of salinity (30 PSU) and decreases as salinity increases or decreases. (Browder et al., 2002; Silva et al., 2010).

If the management measures proposed in this research are implemented, the salinity ranges required for growth and survival of species in Biscayne Bay would be more easily achieved than if salinification is allowed.

4. Conclusions

This research has identified that the year with the lowest annual precipitation (2016) had the least extreme salinity range (15 PSU to 35 PSU), in a 10-year period of analysis. Precipitation during 2016 was evenly distributed throughout the year, suggesting that even modest amounts of freshwater inflows could generate moderate salinity ranges as long as those inflows occur year-round. This has important implications for water management.

In all simulated scenarios, salinity increased most intensely within the central coast of Biscayne Bay. The model estimates that under the mildest scenario (+1.5°C, +0.46 m SLR, +0.6 PSU, +10% increase in precipitation), 50%-increase in baseline freshwater inputs would be required to maintain currently observed salinities in Central Biscayne Bay. Under the worst scenario (+1.5°C, +2.18 m SLR, +0.6 PSU, 10% decrease in precipitation), a 300%-increase of baseline freshwater inputs would be required for the same purpose. This suggests that Everglades Restoration (which aims to restore the salinity of Biscayne Bay to more 'natural' conditions) must consider the effects of climate change and sea level rise. Present strategies may not be sufficient to even maintain current salinity conditions in Biscayne Bay.

Urban greening, groundwater recharge with treated wastewater, and reduction in per capita water consumption are proposed to provide a year-round increase in freshwater inflows to the Bay. These management measures could be transferable to estuaries or coastal locations having similar environmental forcings and governance levels to Biscayne Bay. Water infrastructure investment increases and improvements in water governance structures may be needed to implement those management measures in developing countries.

Acknowledgments

This research was funded by a NOAA/Atlantic Oceanographic and Meteorological Laboratory grant to the Northern Gulf Institute (award number NA160AR4320199).

References

Abd-Elaty, I., Kushwaha, N.L., Grismer, M.E., Elbeltagi, A., Kuriqi, A. (2022). Cost-effective management measures for coastal aquifers affected by saltwater intrusion and climate change (2022). Science of the Total Environment, 836, art. no. 155656. http://doi.org/10.1016/j.scitotenv.2022.155656

Aladejana J.A., Kalin R.M., Sentenac P., Hassan I. (2020). Hydrostratigraphic characterization of shallow coastal aquifers of eastern Dahomey basin, S/W Nigeria, using integrated hydrogeophysical approach; implication for saltwater intrusion. (2020) Geosciences (Switzerland), 10 (2), art. no. 65. https://doi.org/10.3390/geosciences10020065

Alarcon V. J. and Callejas Morales, J. P. (2023) Sustainable land-use/land-cover for stormwater management in three coastal watersheds in central Chile, Urban Water Journal, https://doi.org/10.1080/1573062X.2023.2273543

Alarcon, V. J., Linhoss, A.C., Kelble, C.R. et al. (2022a). Coastal inundation under concurrent mean and extreme sea level rise in Coral Gables, Florida, USA. Nat Hazards 111, 2933–2962 (2022a). https://doi.org/10.1007/s11069-021-05163-0

Alarcon, V.J., Linhoss, A.C., Mickle, P.F., Kelble, C.R., Fine, A. (2022b). Estimation of Groundwater and Salinity for the Central Biscayne Bay Coast, Florida, USA. Lecture Notes in Computer Science, vol 13379. Springer, Cham. https://doi.org/10.1007/978-3-031-10545-6_40

Alexander, M. A., Shin, S.-i., Scott, J. D., Curchitser, E., Stock, C. (2019). The response of the Northwest Atlantic Ocean to climate change. J. Climate 33, 405–428 (2019). https://doi.org/10.1175/JCLI-D-19-0117.1

Aretxabaleta A.L., Smith K.W., Kalra T.S. (2017). Regime changes in global sea surface salinity trend (2017). Journal of Marine Science and Engineering, 5 (4), art. no. 57. https://doi.org/10.3390/jmse5040057

Baldwin, A. H., and Mendelssohn, I. A. (1998). Effects of salinity and water level on coastal marshes: an experimental test of disturbance as a catalyst for vegetation change. Aquatic Botany 61 (1998), pp 255-268.

Basack, S., Loganathan, M. K., Goswami, G., & Khabbaz, H. (2022). Saltwater Intrusion into Coastal Aquifers and Associated Risk Management: Critical Review and Research Directives. Journal of Coastal Research, 38(3), 654–672. https://www.jstor.org/stable/48668657

Berland, A., et al., (2017). The role of trees in urban stormwater management. Landscape and Urban Planning, Volume 162, 2017, Pages 167-177, https://doi.org/10.1016/j.landurbplan.2017.02.017

Bindoff, N.L., W.W.L. Cheung, J.G. Kairo, J. Arístegui, V.A. Guinder, R. Hallberg, N. Hilmi, N. Jiao, M.S. Karim, L. Levin, S. O’Donoghue, S.R. Purca Cuicapusa, B. Rinkevich, T. Suga, A. Tagliabue, and P. Williamson, (2019). Changing Ocean, Marine Ecosystems, and Dependent Communities. In: IPCC Special Report on the Ocean and Cryosphere in a

Changing Climate [H.-O. Pörtner, D.C. Roberts, V. Masson-Delmotte, P. Zhai, M. Tignor, E. Poloczanska, K. Mintenbeck, A. Alegría, M. Nicolai, A. Okem, J. Petzold, B. Rama, N.M. Weyer (eds.)]. Cambridge University Press, Cambridge, UK and New York, NY, USA, pp. 447–587. https://doi.org/10.1017/9781009157964.007

Boretti A. (2019). A realistic expectation of sea level rise in the Mexican Caribbean. Journal of Ocean Engineering and Science, Volume 4, Issue 4, December 2019, Pages 379-386. https://doi.org/10.1016/j.joes.2019.06.003

Browder, J.A., Zein-Eldin, Z., Criales, M.M. et al. Dynamics of pink shrimp (Farfantepenaeus duorarum) recruitment potential in relation to salinity and temperature in Florida Bay. Estuaries 25, 1355–1371 (2002). https://doi.org/10.1007/BF02692230

Butler, S. and Reid, J. (2004). Saltiness of Manatee Habitats Changes with the Seasons. Can That Affect Manatee Migration? https://journeynorth.org/tm/manatee/Salinity.html

Chang, S.W., Clement, T. P., Simpson, M. J., Lee, K. K. (2011). Does sea level rise have an impact on saltwater intrusion? Advances in Water Resources, Volume 34, Issue 10, 2011, pp 1283-1291. https://doi.org/10.1016/j.advwatres.2011.06.006 .

Conrads, P. A. and Darby, L. S. (2017). Development of a Coastal Drought Index Using Salinity. Bulletin of the American Meteorological Society, Vol. 98: Issue 4, pp 753–766. DOI: https://doi.org/10.1175/BAMS-D-15-00171.1

Costa Y., Martins I., de Carvalho G.C., Barros F. (2023). Trends of sea level rise effects on estuaries and estimates of future saline intrusion. (2023) Ocean and Coastal Management, 236, art. no. 106490. https://doi.org/10.1016/j.ocecoaman.2023.106490

Czajkowski, J., Engel, V., Martinez, C., Mirchi, A., Watkins, D., Sukop, M.C., Hughes, J.D. (2018). Economic impacts of urban flooding in South Florida: Potential consequences of managing groundwater to prevent saltwater intrusion (2018). Science of the Total Environment, 621, pp. 465-478. https://doi.org/10.1016/j.scitotenv.2017.10.251

Derkzen, M.L., van Teeffelen, A.J.A. and Verburg, P.H. (2015). Review: Quantifying urban ecosystem services based on high-resolution data of urban green space: an assessment for Rotterdam, the Netherlands. J Appl Ecol, 52: 1020-1032. https://doi.org/10.1111/1365-2664.12469

Dessu, S., Paudel, R., Price, R., Davis, S. (2021). Using empirical data and modeled scenarios of Everglades restoration to understand changes in coastal vulnerability to sea level rise. Climatic Change. 168. https://doi.org/10.1007/s10584-021-03231-9 .

DSI (2017). The Environmental Fluid Dynamics Code: Theoretical & Computational Aspects of EFDC+, Dynamic Solutions - International, LLC, Edmonds, WA, USA, 2017.

Du, J., Park, K. (2019). Estuarine salinity recovery from an extreme precipitation event: Hurricane Harvey in Galveston Bay (2019). Science of the Total Environment, 670, pp. 1049-1059. https://doi.org/10.1016/j.scitotenv.2019.03.265

Elias P. and Omojola A., 2015. Case study: The challenges of climate change for Lagos, Nigeria. Current Opinion in Environmental Sustainability, Volume 13, April 2015, Pages 74-78. https://doi.org/10.1016/j.cosust.2015.02.008

Escolero O.A., Marin L.E., Steinich B., Pacheco J. (2000). Delimitation of a hydrogeological reserve for a city within a karstic aquifer: The Merida, Yucatan example (2000) Landscape and Urban Planning, 51 (1), pp. 53 – 62. https://doi.org/10.1016/S0169-2046(00)00096-7

Geselbracht, L.L., Freeman, K., Birch, A.P., Brenner, J., Gordon, D.R. (2015). Modeled sea level rise impacts on coastal ecosystems at six major estuaries on Florida's gulf coast: Implications for adaptation planning (2015). PLoS ONE, 10 (7), art. no. e0132079. https://doi.org/10.1371/journal.pone.0132079

Goldscheider, N., Chen, Z., Auler, A.S. et al. (2020). Global distribution of carbonate rocks and karst water resources. Hydrogeol J 28, 1661–1677 (2020). https://doi.org/10.1007/s10040-020-02139-5

Harvey, R. G., Squires, M., Beauchamp, J., Mazzotti, F. J., Brandt, L. A. (2016). The American Crocodile: An Indicator Species for Everglades Restoration. University of Florida, Fort Lauderdale Research & Education Center. https://crocdoc.ifas.ufl.edu/publications/factsheets/crocodileindicator.pdf

Herbert, E. R., P. Boon, A. J. Burgin, S. C. Neubauer, R. B. Franklin, M. Ardón, K. N. Hopfensperger, L. P. M. Lamers, and P. Gell. (2015). A global perspective on wetland salinization: ecological consequences of a growing threat to freshwater wetlands. Ecosphere 6(10):206. http://dx.doi.org/10.1890/ES14-00534.1

Hinkel J., Schuerch M., French J., Nicholls R.J. (2023). Sea Level Rise Risk and Adaptation in Estuaries (2023). Climate Change and Estuaries, pp. 581 – 602. http://dx.doi.org10.1201/9781003126096-32

Hochmair, H. H. and Benjamin, A. (2021). Miami-Dade County Urban Tree Canopy Assessment. Geomatics Program at the University of Florida. https://www.miamidade.gov/parks/library/urban-tree-canopy-assessment-2021.pdf

Hollingsworth, E. (2006). Karst regions of the world (KROW): populating global karst datasets and generating maps to advance the understanding of karst occurrence and protection of karst species and habitats worldwide. Thesis, University of Arkansas (2006). https://digital.lib.usf.edu/SFS0052617/00001

Hong, B. and Shen, J. (2012). Responses of estuarine salinity and transport processes to potential future sea level rise in the Chesapeake Bay. Estuarine, Coastal and Shelf Science, Volumes 104–105, 2012, Pages 33-45. https://doi.org/10.1016/j.ecss.2012.03.014

Jasechko, S., Perrone, D., Seybold, H., Fan, Y., Kirchner, J. (2020). Groundwater level observations in 250,000 coastal US wells reveal scope of potential seawater intrusion. Nature Communications. 11. 3229. https://doi.org/10.1038/s41467-020-17038-2

Jones, C. (2009). Temperature and Salinity Tolerances of the Tropical Spiny Lobster, Panulirus ornatus. Journal of World Aquaculture Society 40(6). https://doi.org/10.1111/j.1749-7345.2009.00294.x

Kelble, C., Johns, E., Nuttle, W., Lee, T., Smith, R., Ortner, P. (2007). Salinity patterns of Florida Bay. Estuarine, Coastal and Shelf Science. 71. 318-334. https://doi.org/10.1016/j.ecss.2006.08.006.

Khojasteh D., Lewis M., Tavakoli S., Farzadkhoo M., Felder S., Iglesias G., Glamore W. (2021). Sea level rise will change estuarine tidal energy: A review. (2022) Renewable and Sustainable Energy Reviews, 156, art. no. 111855. https://doi.org/10.1016/j.rser.2021.111855

Knight, T., Price, S., Bowler, D. et al. (2021). How effective is 'greening' of urban areas in reducing human exposure to ground-level ozone concentrations, UV exposure and the 'urban heat island effect'? An updated systematic review. Environmental Evidence 10, 12. https://doi.org/10.1186/s13750-021-00226-y

Knoben, W. J. M., Freer, J. E., Woods, R. A. (2019). Technical note: Inherent benchmark or not? Comparing Nash–Sutcliffe and Kling–Gupta efficiency scores. Hydrol. Earth Syst. Sci., 23, 4323–4331, 2019. https://doi.org/10.5194/hess-23-4323-2019

Langevin C.D. (2003). Simulation of Submarine Ground Water Discharge to a Marine Estuary: Biscayne Bay, Florida (2003). Ground Water, 41 (6), pp. 758 – 771. http://doi.org/10.1111/j.1745-6584.2003.tb02417.x

Luxem, K. (2017). Managed Aquifer Recharge A tool to replenish aquifers and increase underground water storage. https://www.americangeosciences.org/sites/default/files/CI_Factsheet_2017_6_MAR_170921.pdf

Miami-Dade County (2021). Miami-Dade Legislative Item File Number: 211830. https://www.miamidade.gov/global/government/boards/watershed-management-advisory-board.page

Miami Dade Government (2007). Water & Sewer. https://www.miamidade.gov/greenprint/planning/library/milestone_one/water.pdf

Millette, N.C., Kelble, C., Linhoss, A., Ashby, S., Visser, L., 2019. Using Spatial Variability in the Rate of Change of Chlorophyll-a to Improve Water Quality Management in a Subtropical Oligotrophic Estuary (2019). Estuaries and Coasts, 42 (7), pp. 1792-1803. https://doi.org/10.1007/s12237-019-00610-5

Morán-Valencia M., Flegl M., Güemes-Castorena D. (2023). A state-level analysis of the water system management efficiency in Mexico: Two-stage DEA approach. (2023) Water Resources and Industry, 29, art. no. 100200. https://doi.org/10.1016/j.wri.2022.100200

Moriasi, D.N., Arnold, J.G., Van Liew, M.W., Bingner, R.L., Harmel, R.D., Veith, T.L. (2007). Model Evaluation Guidelines for Systematic Quantification of Accuracy in Watershed Simulations. Trans. ASABE 2007, 50, 885–900, https://doi.org/10.13031/2013.23153

National Research Council. 2008. Prospects for Managed Underground Storage of Recoverable Water. Washington, DC. The National Academies Press. https://doi.org/10.17226/12057

NOAA, National Oceanic and Atmospheric Administration (2007). Endangered Species Act: 5-Year Review Johnson's Seagrass (Halophila johnsonii Eiseman). National Marine Fisheries Service. https://www.nrc.gov/docs/ML1224/ML12240A273.pdf

NOAA, National Oceanic and Atmospheric Administration (2005). Coastal Zone Management Act of 1972. https://coast.noaa.gov/data/czm/media/CZMA_10_11_06.pdf

NOAA, National Oceanic and Atmospheric Administration (2018). National Coastal Zone Management Program Strategic Plan 2018-2023. https://coast.noaa.gov/data/docs/czm-strategic-plan.pdf

Nowak D.J., Ellis A., Greenfield E.J. (2022). The disparity in tree cover and ecosystem service values among redlining classes in the United States. (2022) Landscape and Urban Planning, 221, art. no. 104370. https://doi.org/10.1016/j.landurbplan.2022.104370

Nungesser M., Saunders C., Coronado-Molina C., Obeysekera J., Johnson J., McVoy C., Benscoter B. (2015). Potential Effects of Climate Change on Florida's Everglades. (2015) Environmental Management, 55 (4), pp. 824 - 835. https://doi.org/10.1007/s00267-014-0417-5

Oladapo, M. I., Ilori, O. B., Adeoye-Oladapo, O. O. (2014). Geophysical study of saline water intrusion in Lagos municipality. African Journal of Environmental Science and Technology, Vol.8(1), pp. 16-30, January 2014. https://doi.org/10.5897/AJEST2013.1554

Oliveira, A., Fortunato, A.B., Rodrigues, M., Azevedo, A., Rogeiro, J., Bernardo, S., Lavaud, L., Bertin, X., Nahon, A., de Jesus, G., Rocha, M., Lopes, P. (2021). Forecasting contrasting coastal and estuarine hydrodynamics with OPENCoastS. (2021) Environmental Modelling and Software, 143, art. no. 105132. https://doi.org/10.1016/j.envsoft.2021.105132

Pareja-Roman L.F., Chant R.J. (2023). Effects of a Changing Climate on the Physics of Estuaries (2023). Climate Change and Estuaries, pp. 215 – 230. https://doi.org/10.1201/9781003126096-13

Pauleit et al., (2019). Advancing urban green infrastructure in Europe: Outcomes and reflections from the GREEN SURGE project. Urban Forestry & Urban Greening Volume 40, April 2019, Pages 4-16. https://doi.org/10.1016/j.ufug.2018.10.006

Pavelic P., Dillon P.J., Narayan K.A., Herrmann T.N., Barnett S.R. (1997). Integrated groundwater flow and agronomic modelling for management of dryland salinity of a coastal plain in southern Australia. (1997) Agricultural Water Management, 35 (1-2), pp. 75 - 93. https://doi.org/10.1016/S0378-3774(97)00027-9

Poppeschi, C., Charria, G., Goberville, E., Rimmelin-Maury, P., Barrier, N., Petton, S., Unterberger, M., Grossteffan, E., Repecaud, M., Quéméner, L., Theetten, S., Le Roux, J.-F., Tréguer, P. (2021). Unraveling Salinity Extreme Events in Coastal Environments: A Winter Focus on the Bay of Brest (2021). Frontiers in Marine Science, 8, art. no. 705403. https://doi.org/10.3389/fmars.2021.705403

Prinos, Scott. (2016). Saltwater intrusion monitoring in Florida. Florida Scientist, Vol. 79, No. 4, Special Issue: Status of Florida's Groundwater Resources, pp. 269-278. https://www.jstor.org/stable/44113190

Quaranta, E., Dorati, C. & Pistocchi, A. (2021). Water, energy and climate benefits of urban greening throughout Europe under different climatic scenarios. Sci Rep 11, 12163 (2021). https://doi.org/10.1038/s41598-021-88141-7

Reese, R. S. (2002). Inventory and Review of Aquifer Storage and Recovery in Southern Florida, prepared as part of the U.S. Geological Survey Place-Based Studies Program. The U.S. Geological Survey Water Resources Investigation Report 02-4036. Reston, VA: U.S. Geological Survey. https://doi.org/10.3133/wri024036

Robbins, L.L., Lisle, J.T. Regional Acidification Trends in Florida Shellfish Estuaries: a 20+ Year Look at pH, Oxygen, Temperature, and Salinity. Estuaries and Coasts 41, 1268–1281 (2018). https://doi.org/10.1007/s12237-017-0353-8

Rodrigues, M., Rosa, A., Cravo, A., Jacob, J., Fortunato, A. B. (2021). Effects of climate change and anthropogenic pressures in the water quality of a coastal lagoon (Ria Formosa, Portugal). Science of The Total Environment, Volume 780, 2021, 146311, https://doi.org/10.1016/j.scitotenv.2021.146311

Scanes, E., Scanes, P.R. & Ross, P.M. Climate change rapidly warms and acidifies Australian estuaries. Nat Commun 11, 1803 (2020). https://doi.org/10.1038/s41467-020-15550-z

SFWMD, South Florida Water Management District (2021). 2021 South Florida Environmental Report. https://www.sfwmd.gov/sites/default/files/documents/2021_sfer_highlights_hr.pdf

SFWMD, South Florida Water Management District (2020). DBHYDRO (Environmental Data). https://www.sfwmd.gov/science-data/dbhydro

Sastaretsi-Sioui, M. P. (2019). Drought in the Yucatan: Maya perspectives on tradition, change, and adaptation. Current Directions in Water Scarcity Research, Elsevier, Volume 2, 2019, Pages 67-75. https://doi.org/10.1016/B978-0-12-814820-4.00005-5

Shawaqfah M., Almomani F., Al-Rousan T. (2021). Potential Use of Treated Wastewater as Groundwater Recharge Using GIS Techniques and Modeling Tools in Dhuleil-Halabat Well-Field/Jordan. Water. 2021; 13(11):1581. https://doi.org/10.3390/w13111581

Silva E. et al., (2010). Effect of salinity on survival, growth, food consumption and haemolymph osmolality of the pink shrimp Farfantepenaeus subtilis. Aquaculture, Volume 306, Issues 1–4, 2010, Pages 352-356. https://doi.org/10.1016/j.aquaculture.2010.04.025

Silvy, Y., Guilyardi, E., Sallée, J., Durack, P. (2020). Human-induced changes to the global ocean water masses and their time of emergence. Nature Climate Change. https://doi.org/10.10.1038/s41558-020-0878-x

Simpfendorfer, C. (2001). Essential Habitat of smalltooth sawfish (Pristis peetinata). Center for Shark Research. Mote Marine Laboratory, Sarasota, Florida. http://chnep.wateratlas.usf.edu/upload/documents/Essential_habitat_of.pdf

Skliris, N., Marsh, R., Mecking, J.V. et al. (2020). Changing water cycle and freshwater transport in the Atlantic Ocean in observations and CMIP5 models. Clim Dyn 54, 4971–4989 (2020). https://doi.org/10.1007/s00382-020-05261-y

Smart N., Eisenman T.S. and Karvonen A. (2020). Street Tree Density and Distribution: An International Analysis of Five Capital Cities. Front. Ecol. Evol. 8:562646. https://doi.org/10.3389/fevo.2020.562646

Southeast Florida Regional Climate Change Compact Sea Level Rise Work Group (Compact) (2020). Unified Sea Level Rise Projection Southeast Florida: 2019 Update. https://southeastfloridaclimatecompact.org/wp-content/uploads/2020/04/Sea-Level-Rise-Projection-Guidance-Report_FINAL_02212020.pdf

Stabenau, E., Renshaw, A., Luo, J., Kearns, E., Wang, J.D. (2015). Improved coastal hydrodynamic model offers insight into surface and groundwater flow and restoration objectives in Biscayne Bay, Florida, USA (2015). Bulletin of Marine Science, 91 (4), pp. 433-454. http://doi.org/10.5343/bms.2015.1017

Stalker, J.C., Price, R.M. & Swart, P.K. (2009). Determining Spatial and Temporal Inputs of Freshwater, Including Submarine Groundwater Discharge, to a Subtropical Estuary Using Geochemical Tracers, Biscayne Bay, South Florida. Estuaries and Coasts 32, 694–708 (2009). https://doi.org/10.1007/s12237-009-9155-y

Szuts, Z. B., & Meinen, C. S. (2017). Florida Current salinity and salinity transport: Mean and decadal changes. Geophysical Research Letters, 44, 10,495–10,503. https://doi.org/10.1002/2017GL074538

Talke S.A., Jay D.A. (2020). Changing Tides: The Role of Natural and Anthropogenic Factors (2020) Annual Review of Marine Science, 12, pp. 121 – 151. https://doi.org/10.1146/annurev-marine-010419-010727

Thom B., Hudson J., Dean-Jones P. (2023). Estuary contexts and governance models in the new climate era, New South Wales, Australia. (2023) Frontiers in Environmental Science, 11, art. no. 1127839. https://doi.org/10.3389/fenvs.2023.1127839

Timmerman, A., Haasnoot, M., Middelkoop, H., Bouma, T., McEvoy, S., (2021). Ecological consequences of sea level rise and flood protection strategies in shallow coastal systems: A quick-scan barcoding approach (2021) Ocean and Coastal Management, 210, art. no. 105674. https://doi.org/10.1016/j.ocecoaman.2021.105674

Upchurch, S., Scott, T. M., Alfieri, M., Fratesi, B., Dobecki, T. L. (2019). The Karst Systems of Florida: Understanding Karst in a Geologically Young Terrain. Springer, Switzerland (2019), pp 1-15.

Ukpai S.N. (2022). Water policy reform in the Nigeria water governance system: assessment of water resources management based on OECD Principles on Water Governance. (2022) Water Policy, 24 (10), pp. 1704 – 1722. https://doi.org/10.2166/wp.2022.135

Virnstein, R.W. and Morris, L. J. (1996). Seagrass preservation and restoration: A diagnostic plan for the Indian River La-goon. St. Johns River Water Management District. Technical Memorandum No. 14. Palatka, Florida.

Voter, C. B., & Loheide, S. P. (2018). Urban residential surface and subsurface hydrology: Synergistic effects of low-impact features at the parcel scale. Water Resources Research, 54, 8216–8233. https://doi.org/10.1029/2018WR022534

White, E., & Kaplan, D. (2017). Restore or retreat? Saltwater intrusion and water management in coastal wetlands. Ecosystem Health and Sustainability, 3(1), e01258. https://doi.org/10.1002/ehs2.1258

Wang J.D., Luo J., Ault J.S. (2003). Flows, salinity, and some implications for larval transport in South Biscayne Bay, Florida (2003). Bulletin of Marine Science, 72 (3), pp. 695 - 723.

Wilsnack, M.M., Yue, S., Ansar, M.A. (2019). A canal capacity evaluation program for the South Florida water management district (2019). World Environmental and Water Resources Congress 2019: Hydraulics, Waterways, and Water Distribution Systems Analysis - Selected Papers from the World Environmental and Water Resources Congress 2019, pp. 200-207. https://doi.org/10.1061/9780784482353.019

Wu H.C., Felis T., Scholz D., Giry C., Kölling M., Jochum K.P., Scheffers S.R. (2017). Changes to Yucatán Peninsula precipitation associated with salinity and temperature extremes of the Caribbean Sea during the Maya civilization collapse. (2017) Scientific Reports, 7 (1), art. no. 15825. https://doi.org/10.1038/s41598-017-15942-0

Yurek S., Allen M., Eaton M.J., Chagaris D., Reaver N., Martin J., Frederick P., Dehaven M. (2023). Quantifying uncertainty in coastal salinity regime for biological application using quantile regression. (2023) Ecosphere, 14 (4), art. no. e4488. https://doi.org/10.1002/ecs2.4488

Yusuf, M. A. and Abiye T. A. (2019). Risks of groundwater pollution in the coastal areas of Lagos, southwestern Nigeria. Groundwater for Sustainable Development Volume 9, October 2019, 100222. https://doi.org/10.1016/j.gsd.2019.100222

Annex A

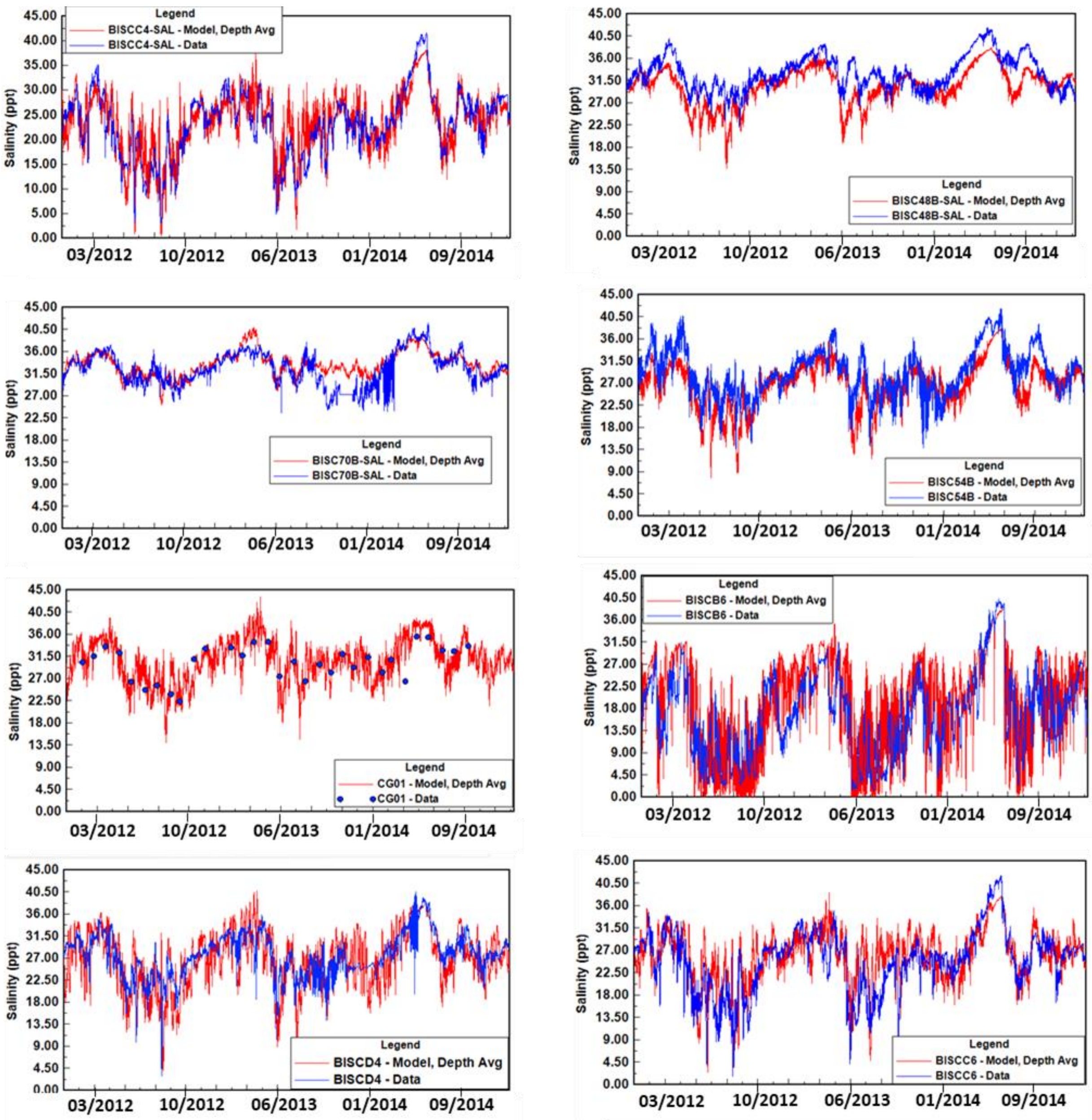

Figure A1. Comparison of observed and simulated hourly salinity during calibration.

Table A1. Statistical fit of simulated salinities during calibration.

Station	Indicators of fit				
	R^2	R	KG	Index of agreement, d	PBIAS
CG01	0.45	0.67	0.67	0.62	1.42
BISC70B	0.57	0.75	0.64	0.65	2.74
BISCD4	0.44	0.67	0.51	0.56	-3.77
BISCC6	0.45	0.67	0.64	0.63	5.11
BISC54B	0.55	0.74	0.73	0.59	-7.92
BISCB6	0.45	0.67	0.63	0.60	16.18
BISCC4	0.69	0.83	0.79	0.70	2.32
BISC48B	0.53	0.73	0.71	0.51	-8.19